

FILE COPY

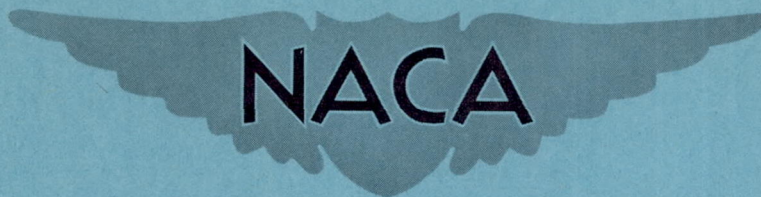
NO 8

RESTRICTED

Copy  
RM E9E12

428

NACA RM E9E12



# RESEARCH MEMORANDUM

EXPERIMENTAL INVESTIGATION OF HOT-GAS BLEEDBACK FOR ICE  
PROTECTION OF TURBOJET ENGINES

III - NACELLE WITH SHORT STRAIGHT AIR INLET

By Robert S. Ruggeri and Edmund E. Callaghan

THIS DOCUMENT ON LOAN FROM THE FILES OF  
Lewis Flight Propulsion Laboratory  
Cleveland, Ohio

NATIONAL ADVISORY COMMITTEE FOR AERONAUTICS  
LANGLEY AERONAUTICAL LABORATORY  
LANGLEY FIELD, HAMPTON, VIRGINIA

CLASSIFICATION CHANGED TO

UNCLASSIFIED

AUTHORITY J. W. CROWLEY

RETURN TO THE ABOVE ADDRESS

CLASSIFIED DOCUMENT

RE-USE OF THIS DOCUMENT FOR PUBLICATIONS SHOULD BE  
AS FOLLOWS:

NATIONAL ADVISORY COMMITTEE FOR AERONAUTICS  
1512 H STREET, N. W.  
WASHINGTON 25, D. C.

This document contains classified information affecting the National Defense of the United States within the meaning of the Espionage Act, 1878. Its transmission or the revelation of its contents in any manner to an unauthorized person is prohibited by law. Information so classified may be imparted only to persons in the military and naval services of the United States, appropriate civilian officers and employees of the Federal Government who have a legitimate interest therein, and to United States citizens of known loyalty and discretion who of necessity must be informed thereof.

DATE 12-14-53 CHANGE #1909 E.L.I

## NATIONAL ADVISORY COMMITTEE FOR AERONAUTICS

WASHINGTON

August 4, 1949

RESTRICTED



## NATIONAL ADVISORY COMMITTEE FOR AERONAUTICS

RESEARCH MEMORANDUMEXPERIMENTAL INVESTIGATION OF HOT-GAS BLEEDBACK FOR ICE  
PROTECTION OF TURBOJET ENGINES

## III - NACELLE WITH SHORT STRAIGHT AIR INLET

By Robert S. Ruggeri and Edmund E. Callaghan

## SUMMARY

Aerodynamic and icing investigations have been conducted in the NACA Lewis icing research tunnel on a two-thirds-scale model of a turbojet-engine nacelle with a short straight air inlet. An investigation of a hot-gas bleedback system consisting of several orifices peripherally located around the inlet was conducted for both dry-air and icing conditions.

The most uniform temperature distribution was obtained at a bleedback of 4.9 percent for a plenum-chamber-gas temperature of 1000° F and yielded an average model-dry-air-temperature rise of 50° F with a maximum deviation from the average model-air-temperature rise of 10° F. For this condition, icing protection was afforded for the inlet screen but not for the accessory housing. Satisfactory agreement between calculated and measured heat requirements was obtained for the icing conditions investigated.

## INTRODUCTION

As part of a general program to provide icing protection for turbojet engines, a nacelle with several air inlets was experimentally investigated in the icing research tunnel of the NACA Lewis laboratory to establish a reasonable design criterion for hot-gas bleedback systems. This investigation is a continuation of the general program outlined in reference 1 and was conducted with the same turbojet-engine nacelle, but with a short straight air inlet.

This short air inlet was used to determine whether sufficient jet mixing would take place to make hot-gas bleedback feasible as a system of ice prevention for this type of installation. The nacelle was two-thirds full scale and the model was provided with orifices



for introducing hot gas into the inlet. Data were obtained to determine the effect of plenum-chamber-gas temperature and pressure, tunnel-air velocity, and angle of attack on the temperature distribution at the simulated engine-inlet screen. The icing investigation to determine the minimum heat requirements was conducted over a range of liquid-water content from 0.7 to 1.4 grams per cubic meter with an average drop diameter of 15 microns. The tunnel total temperature was  $0^{\circ}$  F and the model was investigated at angles of attack of  $0^{\circ}$  and  $8^{\circ}$ .

### APPARATUS

The nacelle investigated was similar to the nacelle described in references 1 and 2, but with a short, circular, and straight air inlet. The model was two-thirds full scale and was constructed of steel, Inconel, and aluminum. The model as installed in the tunnel test section is shown in figure 1. The inlet length from the lip to the accessory housing was 14.0 inches. The inlet area at the lip (leading edge) was 1.952 square feet and the area at the minimum section was 1.124 square feet. The orifices through which the hot gas was discharged were located at the minimum section 3.0 inches from the inlet lip. Hot gas was obtained by passing high-pressure air through a combustion heater and by ducting the gas to the model. A 1/4-inch-mesh, 0.050-inch-diameter wire screen was mounted in the model (fig. 2) to simulate a protective screen installation and to provide a means of indicating icing.

### INSTRUMENTATION

The model instrumentation used in the investigation is shown in figure 2. Measurements were made of mass flow, ram-pressure recovery, pressure drop across the screen, and temperature distribution upstream of the inlet screen.

The average model-air temperature and the temperature distribution inside the model were measured by means of four thermocouple rakes located 33 inches downstream of the orifices and 12 inches upstream of the inlet screen, as shown in figure 2. The thermocouple rakes were spaced at approximately  $90^{\circ}$  intervals around the model and each rake consisted of 16 thermocouple probes spaced 1/4 inch apart.

Aft of the accessory-housing tip the model is the same as that used in the offset and straight air inlet investigations (references 1 and 2). A detailed description of the instrumentation is presented in reference 1.



Temperatures on the surface of the accessory housing were measured by 17 flush-type skin thermocouples.

The state of the gas in the plenum chamber was measured by four thermocouple probes located  $90^\circ$  apart in the plane of the orifices and by four static-pressure taps in the rear wall of the plenum chamber.

The inlet-lip pressure distribution was measured by means of pressure belting cemented to the lip surface. Lip-surface temperatures were measured by thermocouples welded to the inlet lip.

Mass flow through the model and inlet-velocity ratio were controlled by an electrically driven tail cone (fig. 2).

#### PROCEDURE

Aerodynamic investigation without bleedback. - An aerodynamic investigation of the model with orifices was conducted to determine mass-flow characteristics, lip-pressure distribution, and ram-pressure recovery as a function of inlet-velocity ratio and angle of attack. Tunnel-air velocities ranged from approximately 200 to 460 feet per second. At each tunnel-air velocity the angle of attack was varied from  $0^\circ$  to  $8^\circ$  and for each angle of attack the inlet-velocity ratio was varied from 0.68 to 0.89.

Aerodynamic investigation with cold-gas bleedback. - An aerodynamic investigation of the model was conducted to determine the effect of cold-gas bleedback on mass-flow characteristics, lip-pressure distribution, and ram-pressure recovery. This investigation was conducted at an angle of attack of  $0^\circ$  at a fixed tail-cone position corresponding to an inlet-velocity ratio of 0.89 without bleedback. Tunnel-air velocities ranged from 200 to 460 feet per second and bleedbacks ranged from 2.5 to 9.8 percent.

Aerodynamic investigation with hot-gas bleedback. - Several orifice configurations were investigated in order to obtain a configuration that would give the most uniform temperature distribution inside the model for a range of values of tunnel-air velocity, angle of attack, gas flow, and gas temperature. The configuration selected consisted of twelve  $17/32$ -inch-diameter orifices equally spaced around the inlet.

The effect of hot-gas bleedback on the temperature distribution inside the model, mass-flow characteristics, and ram-pressure recovery for the optimum orifice configuration was determined as a



function of tunnel-air velocity, angle of attack, gas flow, and gas temperature. The investigation was conducted at a fixed tail-cone position corresponding to an inlet-velocity ratio of 0.89 without bleedback and at a free-stream total temperature of 0° F for tunnel-air velocities from 200 to 450 feet per second and angles of attack from 0° to 8°. Gas flows and plenum-chamber-gas temperatures ranged from 0.59 to 1.55 pounds per second and from 600° to 1000° F, respectively. For each plenum-chamber-gas temperature, the gas pressure was varied from 3000 to 6000 pounds per square foot absolute.

Icing with hot-gas bleedback. - An investigation to determine the critical icing criterion as a function of mass flow, gas flow, angle of attack, and liquid-water content for a constant free-stream total temperature of 0° F was conducted in a manner similar to that of reference 1. This investigation was conducted at tunnel-air velocities of 200, 275, 355, and 435 feet per second at an angle of attack of 0°. The liquid-water content ranged from 0.70 to 1.4 grams per cubic meter at an average drop diameter of 15 microns. The range of gas flows and plenum-chamber-gas temperatures was the same as those employed for the aerodynamic investigation with hot-gas bleedback.

## RESULTS AND DISCUSSION

### Aerodynamic Investigation without Bleedback

Mass-flow characteristics. - The mass flow through the model increased nearly linearly with tunnel-air velocity for a fixed tail-cone position and angle of attack. A maximum flow of approximately 32.1 pounds per second was obtained at an inlet-velocity ratio of 0.89, a tunnel-air velocity of 460 feet per second, and an angle of attack of 0°.

Ram-pressure recovery. - A ram-pressure recovery of approximately 0.99 was obtained at an angle of attack of 0° and an inlet-velocity ratio of 0.89. Ram-pressure recovery  $\eta$  is defined as

$$\eta = 1 - \frac{P_0 - P_f}{q_0}$$

where

$P_0$  free-stream total pressure, pounds per square foot absolute



$P_f$  total pressure at front rakes, pounds per square foot absolute

$q_0$  free-stream dynamic pressure, pounds per square foot

A decrease in ram-pressure recovery of approximately 1 percent was observed for an increase in angle of attack from  $0^\circ$  to  $8^\circ$ .

Lip-pressure distribution. - The effect of angle of attack on inlet-lip pressure distribution is shown in figure 3. The pressure distribution is presented in terms of a pressure coefficient

$S = 1 - \frac{p - p_0}{q_0}$  where  $p$  is the local surface static pressure in

pounds per square foot absolute and  $p_0$  is the free-stream static pressure in pounds per square foot absolute.

#### Aerodynamic Investigation with Cold-Gas Bleedback

Mass-flow characteristics. - No measurable change in mass flow through the model was observed with increasing cold-gas bleedback.

Ram-pressure recovery. - In order to determine the effect of the jets alone, cold gas was bled into the inlet-air stream. The effect of bleedback on ram-pressure recovery is shown in figure 4 for tunnel-air velocities of 200, 280, 355, and 435 feet per second. The loss in ram-pressure recovery is linearly related to bleedback and no effect of velocity on ram-pressure recovery is evident.

Lip-pressure distribution. - A slight movement of the stagnation point to a position further inside the lip was observed with cold-gas bleedback (fig. 5). This movement increased with increasing bleedback and was caused by the decrease in the inlet-velocity ratio with increasing bleedback, as evidenced by the reduced pressure coefficients in the inlet. The slight change in lip-pressure distribution with bleedback should have a small effect on the external nacelle drag.

No measurable change in mass flow through the model occurred as a result of cold-gas bleedback. A decreasing inlet-velocity ratio must therefore occur with increasing bleedback because an increasing part of the total flow through the model is represented by the bleedback gas and as a consequence the air flow entering the inlet is reduced.



## Aerodynamic Investigation with Hot-Gas Bleedback

Optimum orifice configuration. - The results presented herein are for the orifice configuration that gave the most uniform temperature distribution at the calculated value of bleedback (4.9 percent) and plenum-chamber-gas temperature ( $1000^{\circ}\text{F}$ ) necessary for adequate ice prevention corresponding to an icing condition of 1.4 grams per cubic meter at a tunnel total temperature of  $0^{\circ}\text{F}$ . Preliminary computations utilizing the equations and the method of reference 2 showed the impracticality of providing ice protection for the accessory housing. Because of the large inlet diameter and the short mixing distance (11 in.) from the orifices to the accessory-housing tip, extremely large-diameter orifices would be required to obtain adequate jet penetration. Inasmuch as these large-diameter orifices would necessarily be few in number in order to pass only the required amount of bleedback gas, the temperature distribution inside the model would be very poor.

The investigation was therefore undertaken with the purpose of providing ice protection only for the inlet screen under the most severe conditions used in the icing investigation. By use of the method of reference 2 and assuming that the depth of penetration of the jets required at the screen was one-half of the duct diameter at the accessory-housing tip, an orifice diameter of 0.52 inch was obtained at the design conditions for the model. The model was designed to handle 31 pounds of air per second at a tunnel-air velocity of 425 feet per second and a free-stream density of 0.0024 slug per cubic foot. The calculated total jet area required to pass the required amount of bleedback gas (1.38 lb/sec at maximum air flow through the model) was 2.65 square inches. The results of reference 2 indicate that for a circular inlet, a minimum of 12 orifice holes are required to obtain a good temperature distribution inside the model. In order to obtain the required total jet area with the minimum number of orifices, a configuration consisting of 12 orifices of 17/32-inch diameter equally spaced around the inlet was used in the investigation. This configuration gave the most uniform temperature distribution inside the model for the calculated values of bleedback and plenum-chamber-gas temperatures required for ice prevention.

In order to be certain that the orifice configuration found by the method of reference 2 was the best, several other configurations were experimentally investigated. A configuration consisting of nine equally spaced 5/8-inch-diameter orifices was investigated. The results showed that, although greater penetrations were obtained than with the 12-orifice configuration, the local-air-temperature



deviations inside the model were greater. Another configuration consisting of 16 orifices of 15/32-inch diameter was also investigated. The best temperature distribution obtained with this configuration was slightly inferior to the optimum temperature distribution obtained with the 12-orifice configuration. The best temperature distribution with the 16-orifice configuration was obtained at higher than the calculated value of bleedback, which resulted when high plenum-chamber-gas pressures were employed in order to obtain adequate penetration.

Model-air-temperature distribution. - Once the optimum temperature distribution inside the model was obtained at the calculated value of bleedback, it could be maintained for a range of tunnel-air velocities provided that the bleedback was held constant. The plenum-chamber-gas pressure corresponding to the optimum temperature distribution varied linearly with tunnel-air velocity, as in reference 2. This variation of plenum-chamber-gas pressure with tunnel-air velocity for the optimum temperature distribution is shown in figure 6 for a plenum-chamber-gas temperature of 1000° F. For the curve shown, the bleedback in each case was approximately 4.9 percent, which yielded average model-air-temperature rises of 50° F.

Although the radial temperature distribution observed on each thermocouple rake was very good and the maximum deviation from the average temperature for the rake was only 2° to 4° F; when the temperatures of all thermocouple rakes were considered, the maximum temperature deviation was 9° to 10° F. This rather large temperature variation resulted from incomplete jet mixing at the simulated inlet screen, as evidenced by the fact that the average air temperature measured on a thermocouple rake located directly downstream of an orifice was higher than the average model-air temperature; whereas the temperature measured on a thermocouple rake located between orifices was consistently lower than the average model-air temperature. Mixing of the hot gases with the inlet air was apparently suppressed by the converging annulus formed by the accessory housing and the outer duct wall.

The use of plenum-chamber-gas pressures corresponding to the optimum temperature distribution inside the model gave insufficient penetration to provide adequate ice protection for the accessory-housing tip. Temperature distributions on the accessory housing for several values of hot-gas bleedback at a plenum-chamber-gas temperature of 1000° F and a tunnel-air velocity of 200 feet per second are shown in figure 7. A bleedback of approximately 6.0 percent would be required for complete icing protection of the accessory housing for this tunnel-air velocity (fig. 7). The use



of plenum-chamber-gas pressures higher than the optimum resulted in higher temperatures near the accessory housing with lower air temperatures near the outer duct wall. The use of plenum-chamber-gas pressures lower than optimum resulted in low air temperatures near the accessory-housing skin with increased model-air temperatures near the duct wall.

The effect of angle of attack on the temperature distribution inside the model was negligible.

Increasing the plenum-chamber-gas temperature at a fixed angle of attack had very little effect on the temperature distribution at the inlet screen aside from increasing the temperature level.

Mass-flow loss. - A reduction in mass flow through the model occurred with increasing model-air temperature at fixed tunnel-air velocity, tunnel-air temperature, and angle of attack. The decrease in mass flow with increasing model-air temperature for several values of tunnel-air velocity and an angle of attack of  $0^\circ$  is shown in figure 8. The decrease in mass flow is linearly related to the model-air-temperature rise, but does not vary directly with decreasing model-air density associated with increasing temperature, as shown in figure 8. Thus, the model did not operate as a constant-volume machine as did the models previously investigated (references 1 and 2); instead the experimental mass-flow curve falls between the constant-mass-flow and constant-volume curves.

Ram-pressure recovery. - The ram-pressure loss associated with the addition of heat by jets directed perpendicularly to a moving air stream consists of two components. The first component arises from the momentum pressure loss associated with changing the direction of the jets. The other component arises from the change in density of the air due to the addition of heat. The effect of the first component is illustrated in figure 4.

The variation of ram-pressure recovery with model-air-temperature rise is shown in figure 9. The ram-pressure recovery decreased linearly with increasing model-air-temperature rise. A comparison of figures 4 and 9 with data from references 1 and 2 showed that the ram-pressure recoveries observed with heat addition during this investigation were considerably higher than those obtained in previous investigations and were caused by the model having operating characteristics between those of a constant-mass-flow and a constant-volume machine. As a result, the ram-pressure recoveries with heat addition approached those obtained with cold-gas bleedback.



Inlet-lip temperature distribution. - The maximum inlet-lip temperatures were obtained at the highest value of bleedback (9.1 percent) and plenum-chamber-gas temperature (1000° F) utilized in the investigation. The variation of inlet-lip temperature distribution with hot-gas bleedback is shown in figure 10 for a plenum-chamber-gas temperature of 1000° F and a tunnel-air velocity of 205 feet per second. The inlet-lip temperatures decreased with decreasing bleedback, increasing tunnel-air velocity, or decreasing plenum-chamber-gas temperature.

#### Icing with Bleedback

In analyzing the icing data, the pressure-drop coefficients  $\Delta p/q$  across the screen were computed for each icing run where  $\Delta p$  is the static-pressure drop across the screen and  $q$  is the dynamic pressure upstream of the screen. The screen was considered iced when the value of  $\Delta p/q$  approached 1.5 times the value for the screen at the beginning of each run. The experimental bleedback and plenum-chamber-gas temperatures corresponding to this criterion are shown in figure 11 for tunnel-air velocities of 200, 275, 355, and 435 feet per second at an angle of attack of 0°.

The theoretical curves shown in figure 11 are based on the assumption that icing occurs when the minimum adiabatic wall temperature or kinetic temperature (static temperature plus 0.85 times the dynamic temperature) on the screen was 32° F. These curves represent the upper and lower limits of the icing conditions used in the investigation; that is, curve A was calculated for saturated air at 0° F, a tunnel-air velocity of 435 feet per second, and a liquid-water content of 1.4 grams per cubic meter. Curve B was calculated for saturated air at 0° F, a tunnel-air velocity of 200 feet per second, and a liquid-water content of 0.7 gram per cubic meter.

In order to assure a minimum adiabatic wall temperature of 32° F on the screen, an average adiabatic wall temperature of 42° F and a total temperature of 45.9° F are required at a tunnel-air velocity of 435 feet per second, corresponding to a velocity in the screen of 558 feet per second and a total temperature of 43.1° F at a tunnel-air velocity of 200 feet per second, corresponding to a velocity in the screen of 295 feet per second.

The data in figure 11 fall within the limits of the two curves. The displacement of some of the high-velocity data from curve A and the low-velocity data from curve B was due to the variation in liquid-water content and the use of other than the optimum amount of bleedback.



For all icing conditions investigated, icing of the accessory housing occurred at bleedbacks less than approximately 6.0 percent for a plenum-chamber-gas temperature of 1000° F. The largest ice formation observed on the accessory housing was an ice cap 4 inches in diameter and  $3\frac{1}{2}$  inches thick with some ice extending back 7 inches along the skin. This ice accretion formed during a 40-minute icing period in which the bleedback was reduced from an initial value of 5.6 percent to a final value of 4.9 percent at a constant plenum-chamber-gas temperature of 1000° F. The icing condition was at a tunnel total temperature of 0° F and liquid-water content of 0.75 gram per cubic meter. No ice formations were observed on the duct walls for the conditions investigated.

The importance of accessory-housing ice protection depends largely on the particular jet engine to be used. If protection is essential, the accessory housing cover may be heated either by hot gases or electrically.

#### SUMMARY OF RESULTS

The following results were obtained from an aerodynamic and icing investigation in the icing research tunnel of a two-thirds-scale model of a turbojet-engine nacelle with a short straight air inlet utilizing a hot-gas bleedback system for ice prevention:

1. The optimum temperature distribution was obtained at a bleedback of 4.9 percent and was independent of tunnel-air velocity. This value of bleedback resulted in an average model-dry-air-temperature rise of 50° F with a maximum local temperature deviation of 10° F at the inlet screen for a plenum-chamber-gas temperature of 1000° F.
2. The use of plenum-chamber-gas pressure other than optimum resulted in increased temperature gradients across the inlet. For pressures higher than optimum, low-temperature regions existed near the duct walls; for pressures lower than optimum, low-temperature regions occurred at accessory-housing skin.
3. The introduction of cold gas under pressure through the orifices decreased the ram-pressure recovery linearly with increasing bleedback.
4. Hot-gas bleedback decreased the ram-pressure recovery linearly with increasing model-air temperature rise.



5. For a constant tunnel-air velocity, the mass flow through the model decreased linearly with increasing model-air-temperature rise.

6. Satisfactory agreement between the measured and calculated heat requirements for icing conditions was obtained.

7. Icing protection for the accessory housing could be obtained at bleedbacks greater than 6.0 percent for a plenum-chamber-gas temperature of  $1000^{\circ}$  F.

Lewis Flight Propulsion Laboratory,  
National Advisory Committee for Aeronautics,  
Cleveland, Ohio.

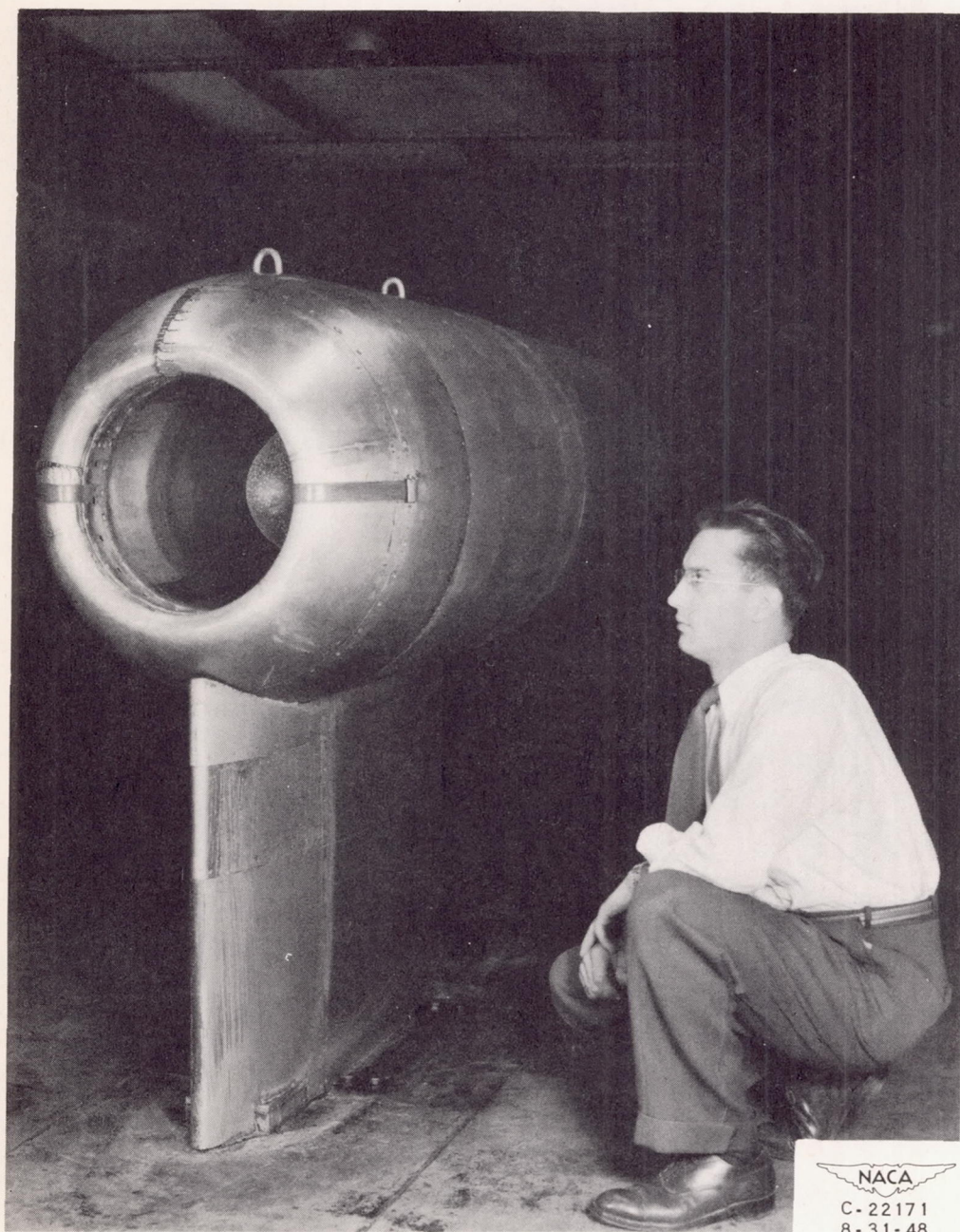
#### REFERENCES

1. Callaghan, Edmund E., Ruggeri, Robert S., and Krebs, Richard P.: Experimental Investigation of Hot-Gas Bleedback for Ice Protection of Turbojet Engines. I - Nacelle with Offset Air Inlet. NACA RM E8D13, 1948.
2. Callaghan, Edmund E., and Ruggeri, Robert S.: Experimental Investigation of Hot-Gas Bleedback for Ice Protection of Turbojet Engines. II - Nacelle with Long Straight Air Inlet. NACA RM E9C16, 1949.





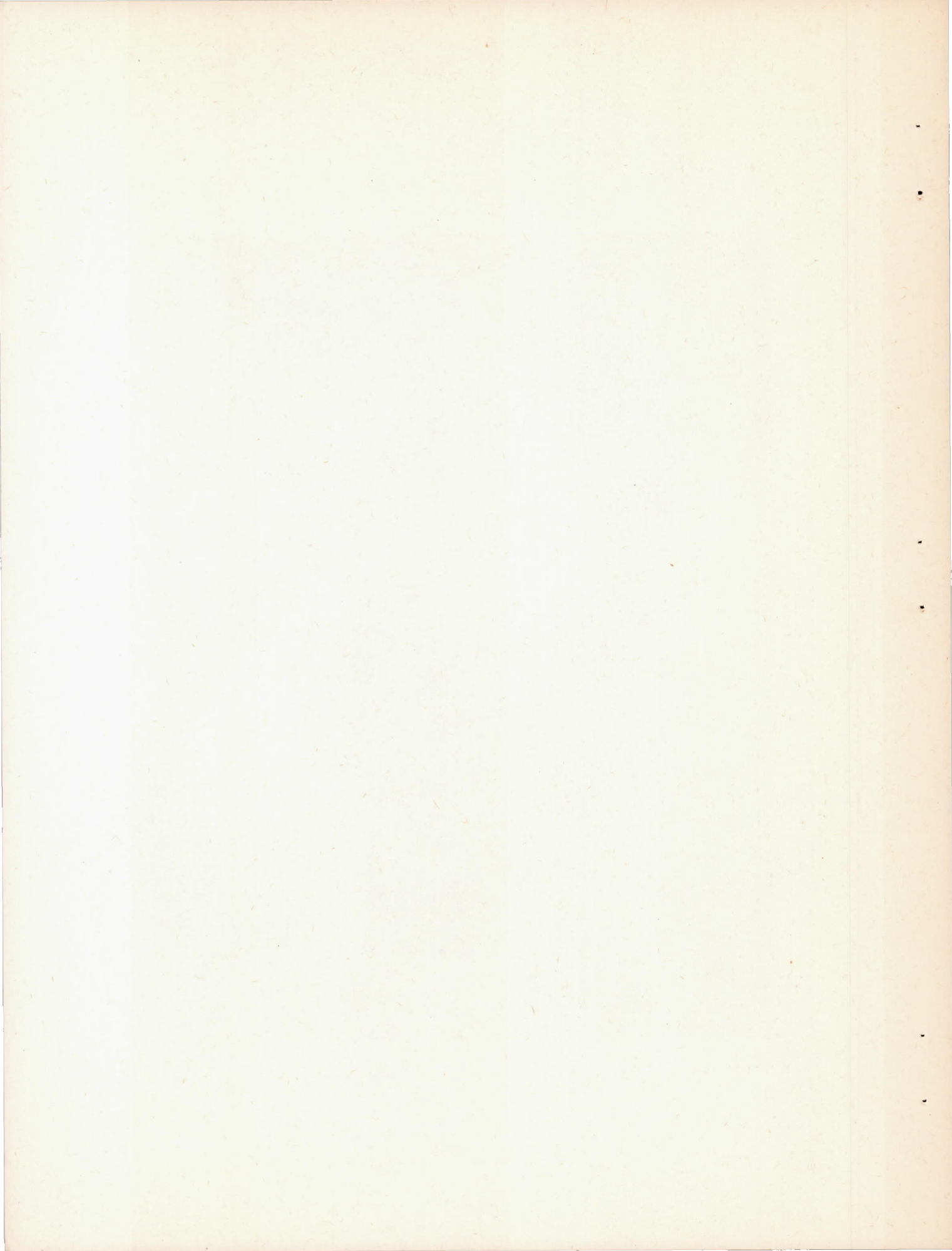




NACA  
C-22171  
8-31-48

Figure 1. - Photograph of model installation in tunnel test section.







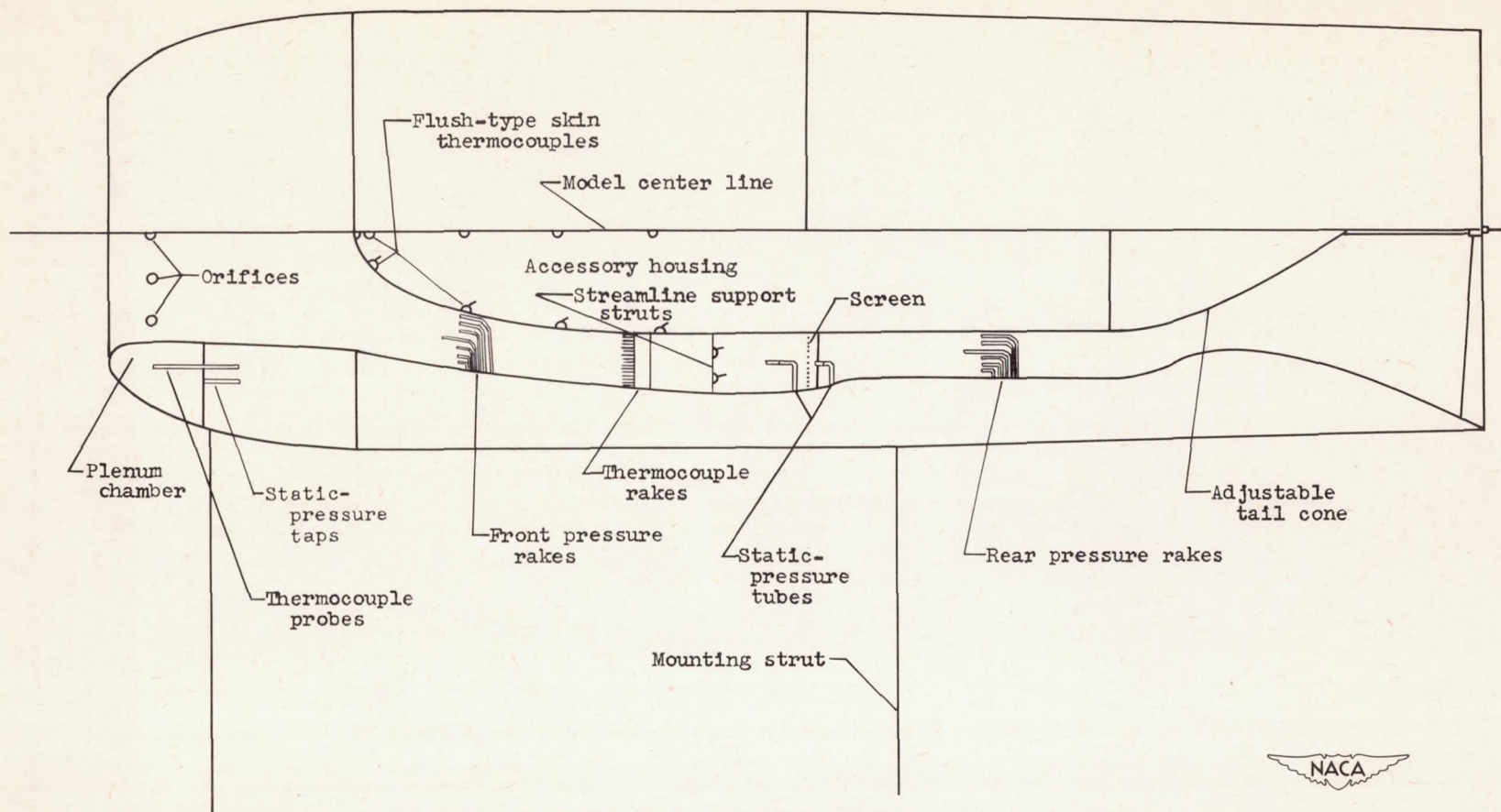
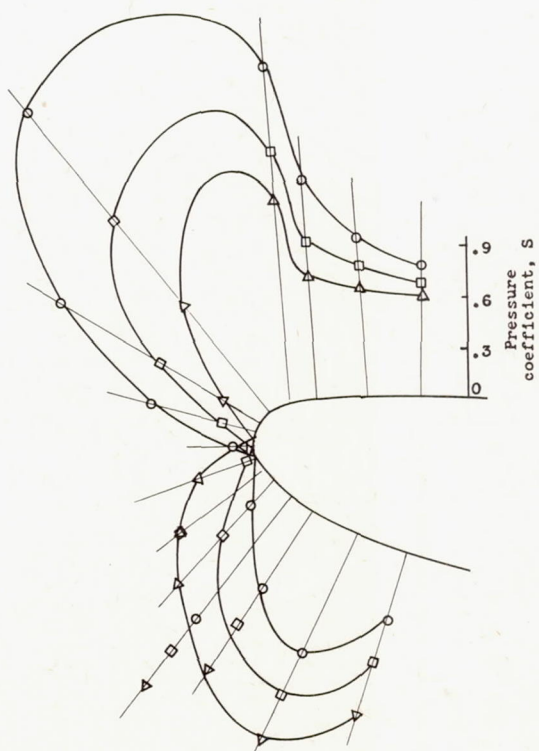
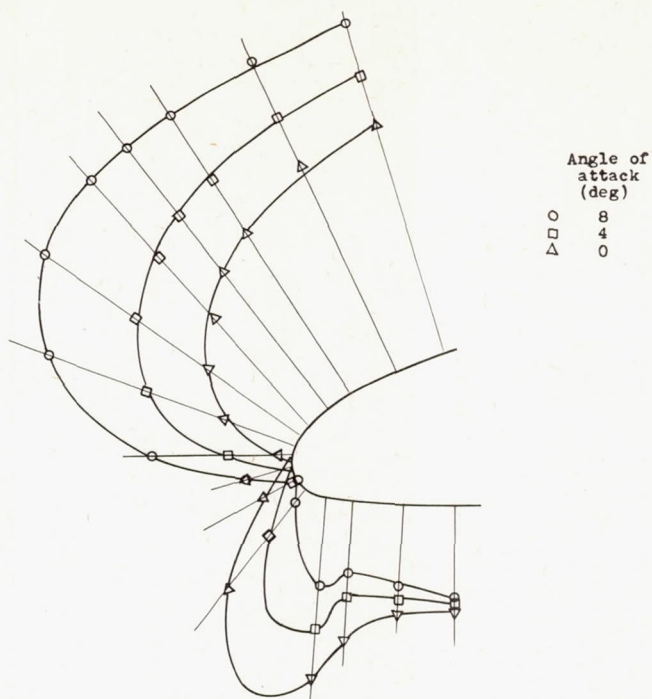


Figure 2. - Sketch of model showing instrumentation used in investigation.





NACA

Figure 3. - Effect of angle of attack on inlet-lip pressure distribution.



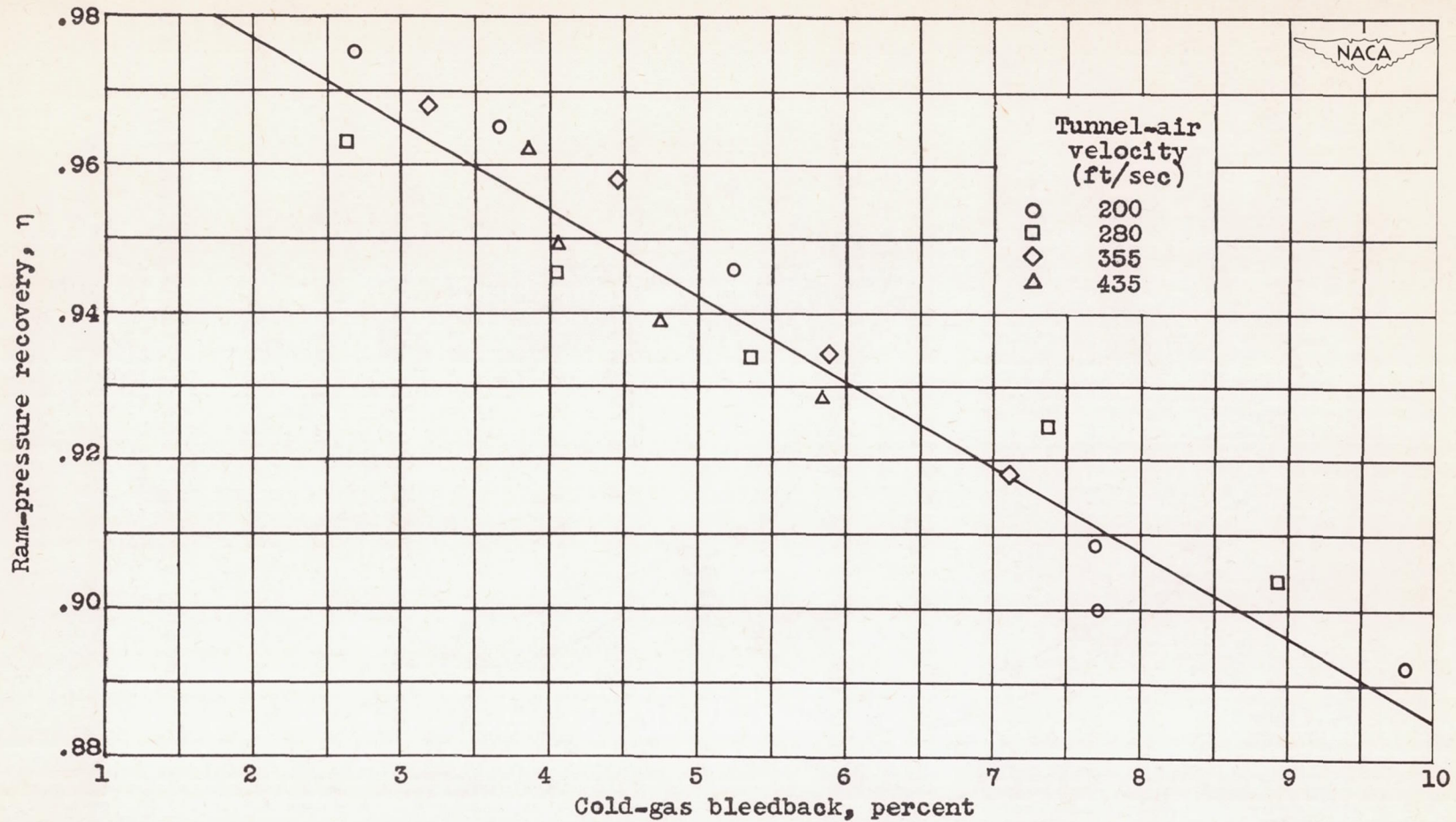


Figure 4. - Variation of ram-pressure recovery with cold-gas bleedback. Angle of attack,  $0^\circ$ .



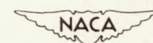
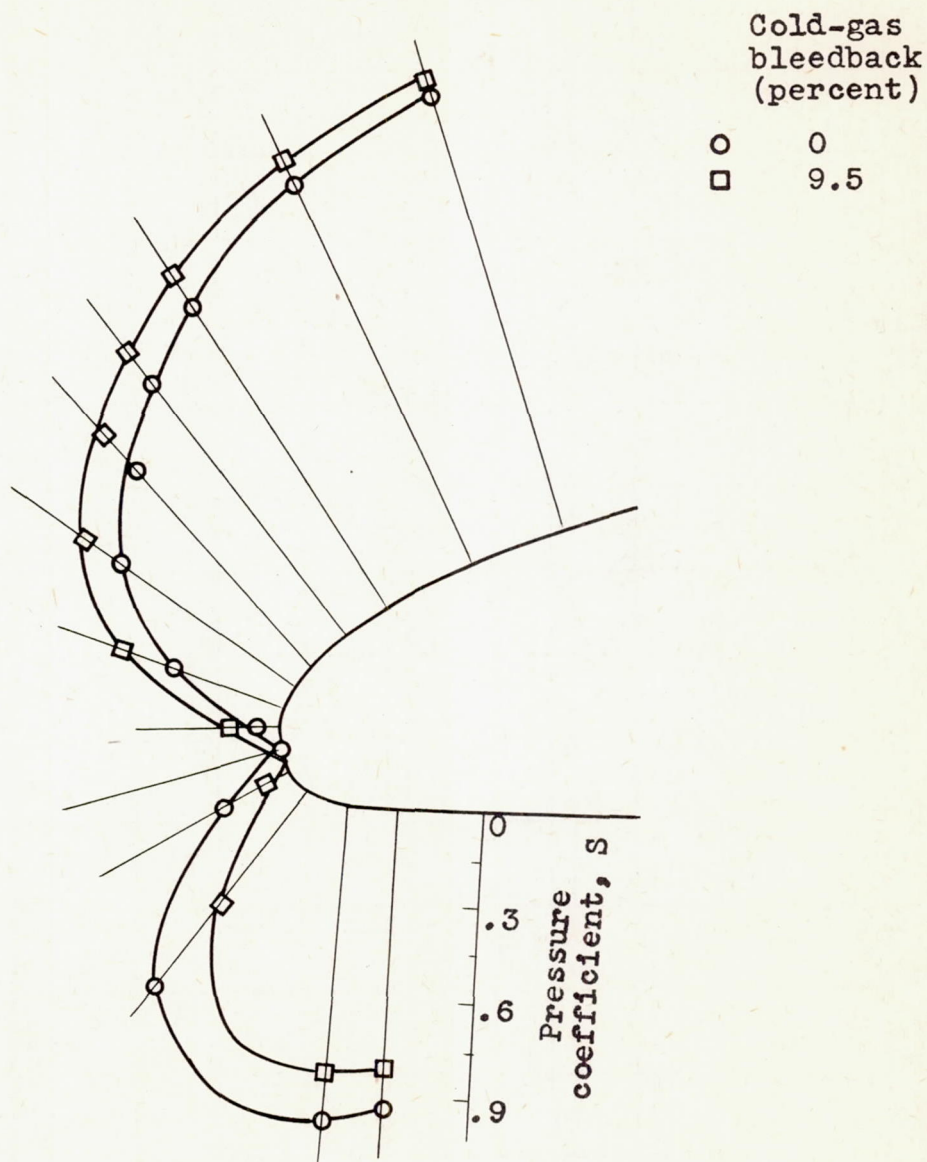


Figure 5. - Effect of cold-gas bleedback on inlet-lip pressure distribution.



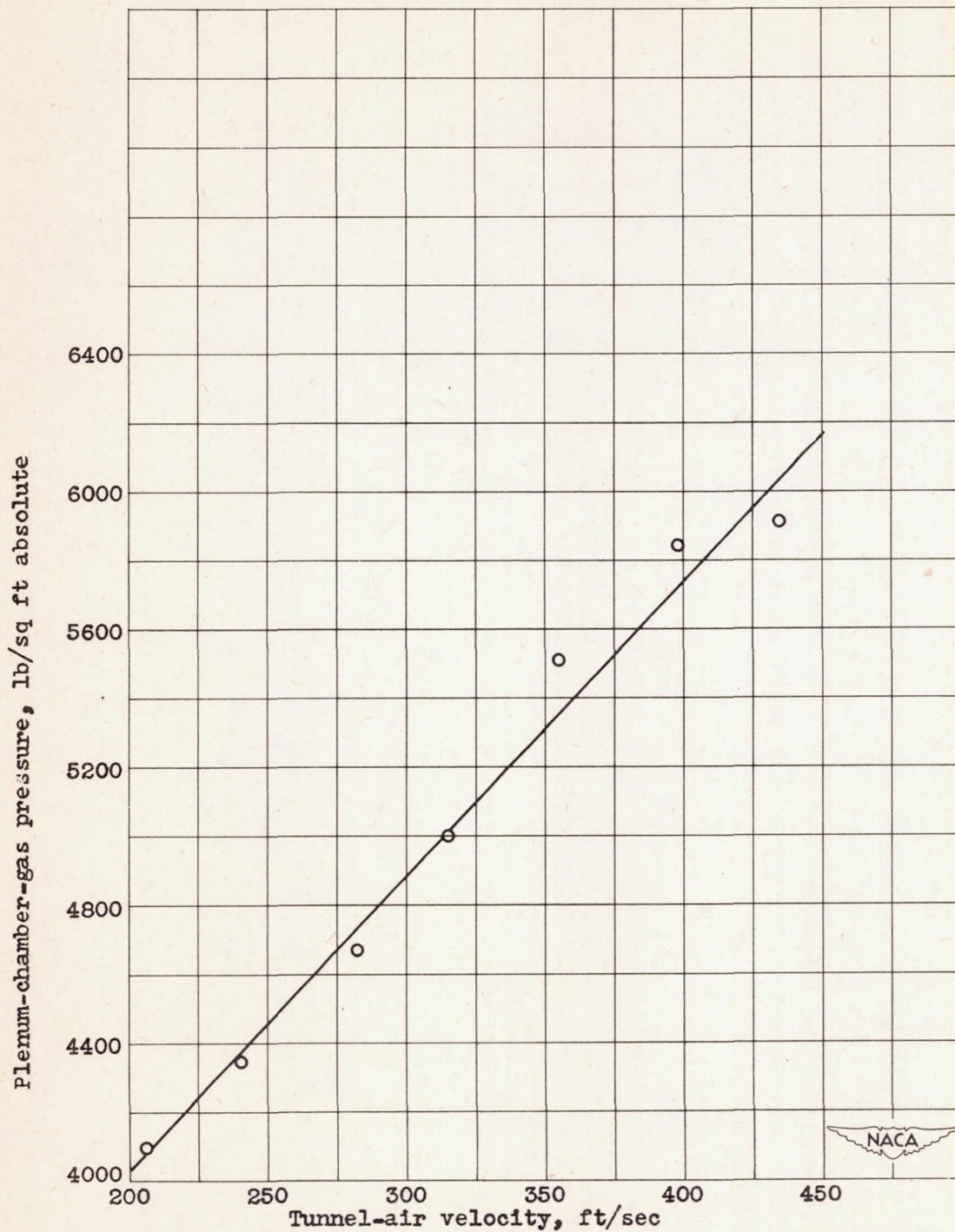


Figure 6. - Relation between plenum-chamber-gas pressure and tunnel-air velocity corresponding to optimum temperature distribution in model. Bleedback, 4.9 percent; plenum-chamber-gas temperature, 1000° F; average model-air-temperature rise, 50° F.



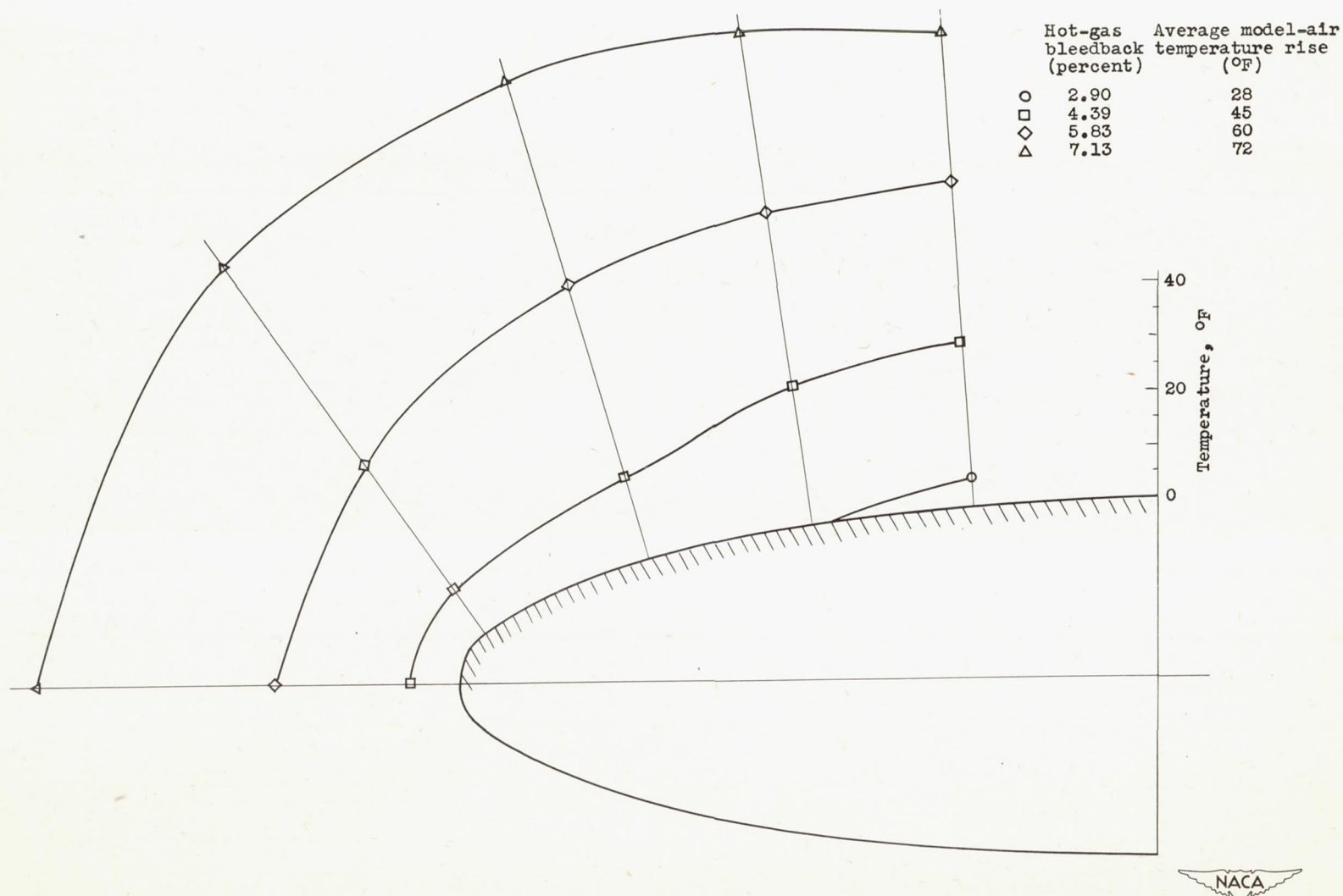
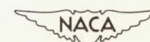


Figure 7. - Temperature distributions measured on accessory housing for several values of hot-gas bleedback. Plenum-chamber-gas temperature, 1000° F; tunnel-air velocity, 200 feet per second; tunnel total temperature, 0° F.





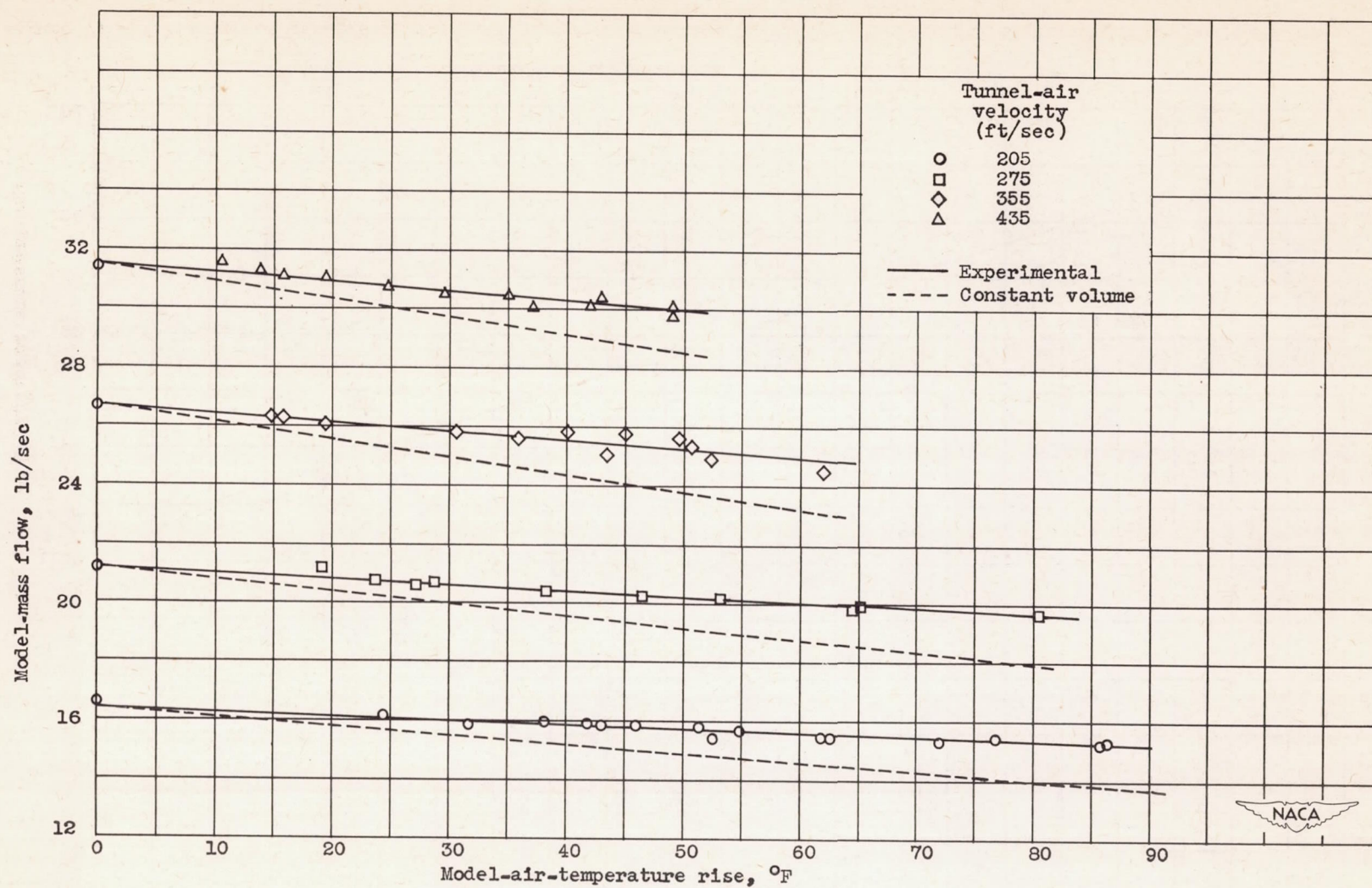


Figure 8. - Variation of model-mass flow with model-air-temperature rise for several tunnel-air velocities. Angle of attack, 0°; tunnel total temperature, 0° F.



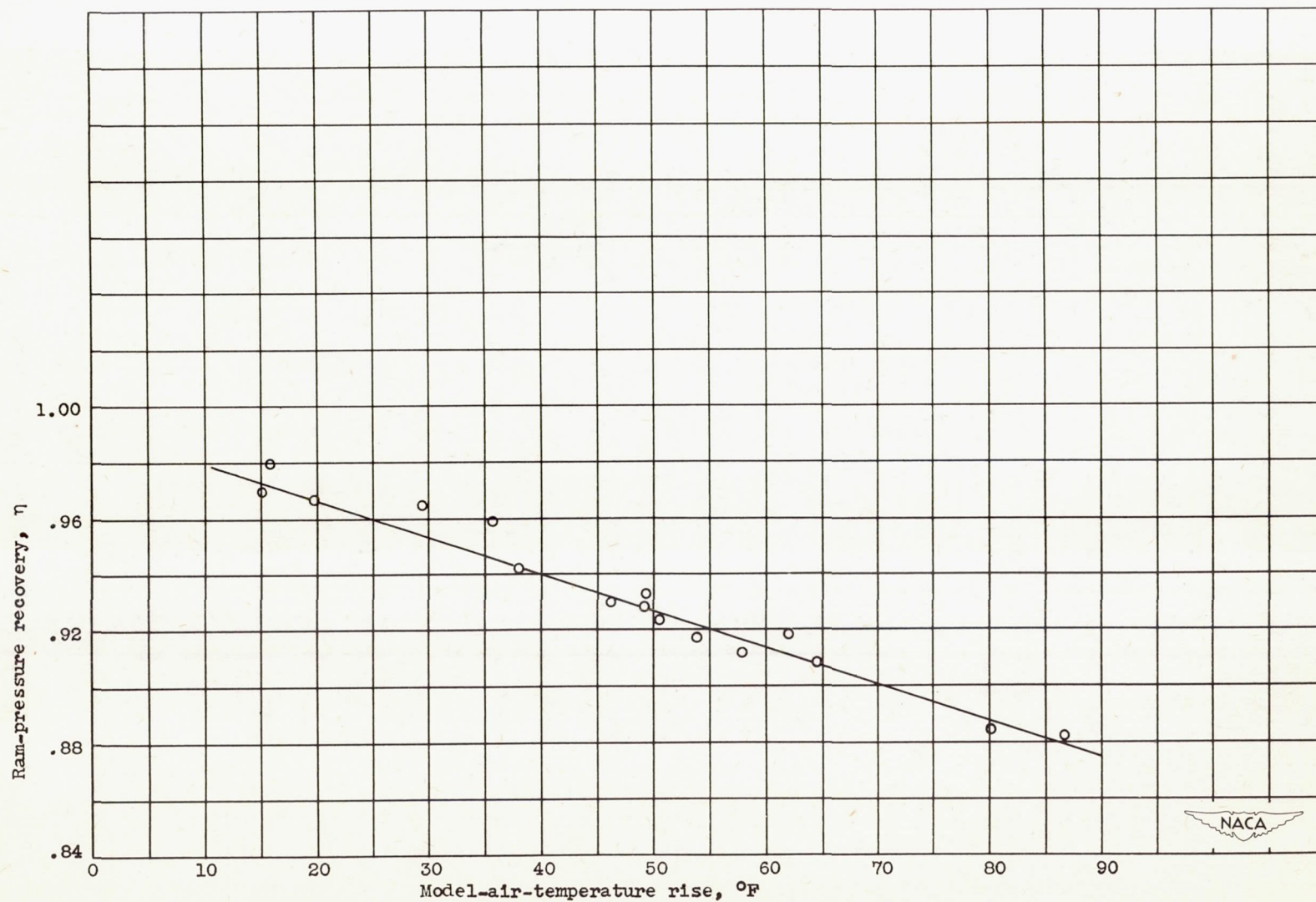


Figure 9. - Variation of ram-pressure recovery with model-air-temperature rise. Angle of attack,  $0^{\circ}$ ; plenum-chamber-gas temperature,  $1000^{\circ}\text{F}$ .



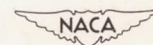
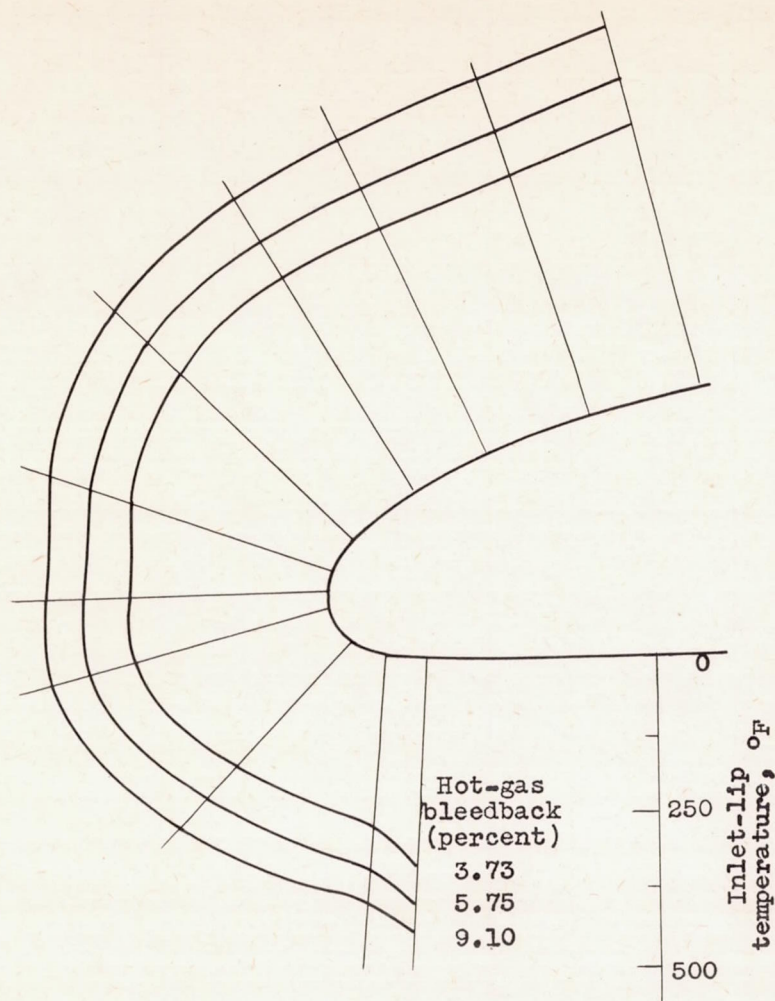


Figure 10. - Variation of inlet-lip temperature distribution with hot-gas bleedback. Plenum-chamber-gas temperature, 1000° F; tunnel-air velocity, 205 feet per second; tunnel total temperature, 0° F; angle of attack, 0°.



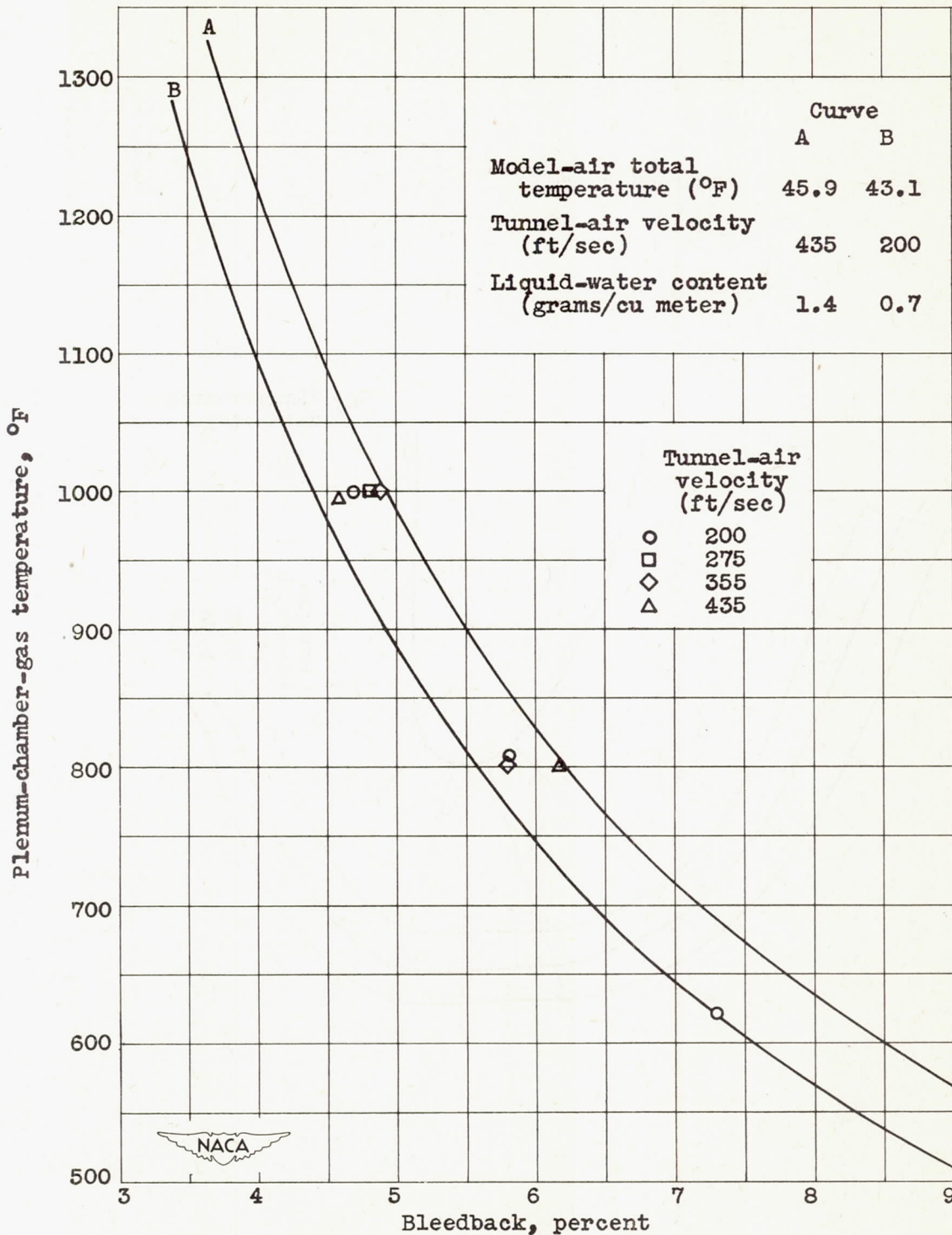


Figure 11. - Bleedback required for ice prevention as function of plenum-chamber-gas temperature for tunnel total temperature of 0° F.